

## Chapter

# Effect of Welding Variables on the Quality of Weldments

*Ramy A. Fouad, Essam Ahmed Ali,*

*Ahmed Ramadan Shaaban and Ahmed E. El-Nikhaily*

## Abstract

The effect of nitrogen addition, heat input, and filler metals on weld metal microstructure and mechanical properties of alloy 316 ASS are studied. Autogenous gas tungsten arc welding (GTAW) is employed by adding up to 2vol. % N<sub>2</sub> in Ar. These variables affect a number of welding aspects, including arc characteristics and microstructure. The influence of shielding gas mixtures on microstructure and mechanical properties of GTAW of austenitic 316 stainless steel is studied. Mechanical properties of welds are determined through uniaxial tension, hardness measurements, impact, and bending tests. Weld defects, as porosity and inclusions are examined using radiographic testing. Weld specimens are free of porosity, inclusions, and hydrogen cracking. Mechanical properties and cooling rate are lower at higher heat input, but the cooling time, nugget area, and solidification time are higher. The addition of N<sub>2</sub> to Ar shielding gas leads to higher values of the ultimate tensile strength 'UTS', yield stress 'YS', and elongation percent. UTS, YS, and elongation of welds depend on heat input, filler metal, and N<sub>2</sub> content of shielding gas. Finally, a mathematical model is built depending upon the welding current, filler metals, and shielding gases.

**Keywords:** TIG welding, filler metals, nugget area, cooling rate, welding variables

## 1. Introduction

In this chapter, we will first introduce you to the field of welding processes using different welding variables examples. We will then provide an introduction to the classification of welding variables. Although most engineering programs or mechanical engineering programs require students to take welding technology courses, you should approach your study of welding technology as more than a mere requirement. Thorough knowledge of welding processes will make you a better engineer and designer. Welding science underlies all technological advances and an understanding of the basics of welding and its applications will not only make you a better engineer but will help you during the production process. In order to be a perfect designer, you must learn what welding will be appropriate to use in different applications. Also, in this chapter, previous works related to the current study are discussed. Various welding techniques will be presented. Finally, studies focused on welding and the effect of welding variables on stainless steel will be discussed. GTAW is considered

one of the most productive welding methods since it is used in the welding of metals with high thickness. For this reason, it is used in the heavy industry and shipbuilding industry.

The shielding gas interacts with the base material and with the filler material, if any, to produce the basic strength, toughness, and corrosion resistance of the weld. It also affects weld bead shape and penetration pattern [1, 2]. Successful GTAW weldments of Monel 400 and AISI 304 were developed using ER304, ERNiCrMo-3, and ERNiCrMo-4 welding wires [3]. The tensile strength and yield strength of ERNiCrMo-3 weldments were comparable to those of parent metals. Tensile strength and yield stress of dissimilar ERNiCrMo-3 weld joints were better than ER304 and ERNiCrMo-4 weldments. Also, the effect of welding wires on the characteristics of dissimilar welding of SS316 L and carbon steel A516 GR 70 was studied [4] using three different filler materials ER80-Ni1, ER309L, and ER NiCrMO-3 (Inconel 625). Inconel 625 was found more suitable to weld dissimilar SS316 L and carbon steel A516 GR 70. Best results concerning UTS, and hardness were obtained using Inconel 625 as a welding electrode. The effect of welding electrodes on the characteristics of dissimilar AISI 420 and 304 L welds was studied [5] using three different filler rods ER312, ER316 L, and ER2209. The last rod produced welds with the highest impact toughness and lowest hardness. Kanigalpula et al. [6] developed mathematical models using central composite design methodology 'CCD' to determine the process variables that produce more stable weld bead geometry and microhardness in the electron beam welding process. Hackenhaar et al. [7] applied Box-Behnken design 'BBD' to investigate the effect of gas metal arc welding 'GMAW' parameters (wire feed speed, welding speed, and arc voltage) based on 3 responses (melting efficiency, bead on plate, and melting area of T-joint) in GTAW butt welding of 6.35 mm thick AISI 1010 steel plates. The melting efficiency showed a direct relationship with heat flow extraction in weld joint, thus, of joint geometry. Melting efficiency is lower for T-joint regardless used equation.

## 2. Basic welding parameters

The welding arc is formed by the arc plasma, which consists of ionized gas, molten metals, slags, vapors, and gaseous atoms and molecules. Arc welding variables are welding current, arc voltage, welding speed, shielding gas and filler metal that cause much more effect on various weld joint properties such as strength, weld bead geometry, cooling rate and corrosion of stainless steel.

### 2.1 Welding current

Welding current is the most important variable affecting melting rate, metal deposition rate, depth of penetration, width of joint and the amount of molten base metal. The electrical energy can be calculated by Eq. (1) [8]:

$$Q = I * V \text{ J/S or } Q = I^2 * R_a \text{ J/S} \quad (1)$$

where, Q = Consumed electrical energy I = Welding current.

V = Arc voltage  $R_a$  = Arc resistance.

The influence of welding current on AISI 316 welded by GTA was studied [9]. UTS and HV increased with increasing heat input. Best results for UTS and HV were

obtained using 100A. Also, sigma phase and  $Cr_{23}C_6$  in 316 SS welded samples increased with increasing heat input as shown in **Figures 1–3**.

### 2.1.1 Welding arc voltage

Welding arc voltage or arc voltage is the electrical potential difference between the welding wire tip and the molten weld zone surface. The welding arc voltage depends on arc length and type of electrode. Weld bead shape appearance depends on arc voltage. Increasing arc voltage causes porosity, welding reinforcement electrode, spatter flatten the weld bead, and increases the weld width [10].

### 2.1.2 Gas purity

Metals differ in their tolerance for foreign components of the shielding gas. Impurities of shielding gases affect weld quality and eventual fitness. Basyigit and Kurt [11] employed five different shielding gases such as, pure argon, 99%Ar + 1%  $N_2$ , 97%

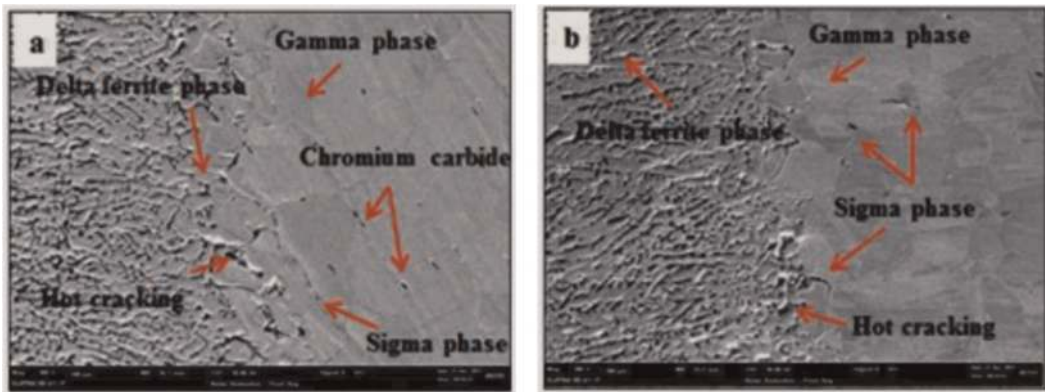


**Figure 1.** Effects of welding current on the sigma and carbide phases distribution of 316 stainless steel, achieved by FESEM – EDX (a) current 90A and (b) current 110A.

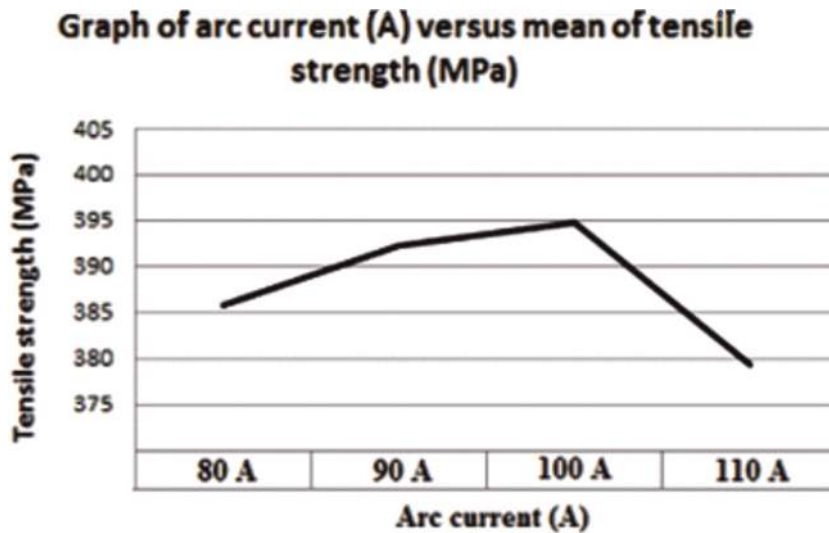


**Figure 2.** Graph of arc current (A) versus mean of tensile strength (MPa) for 316 stainless steel welded joint.

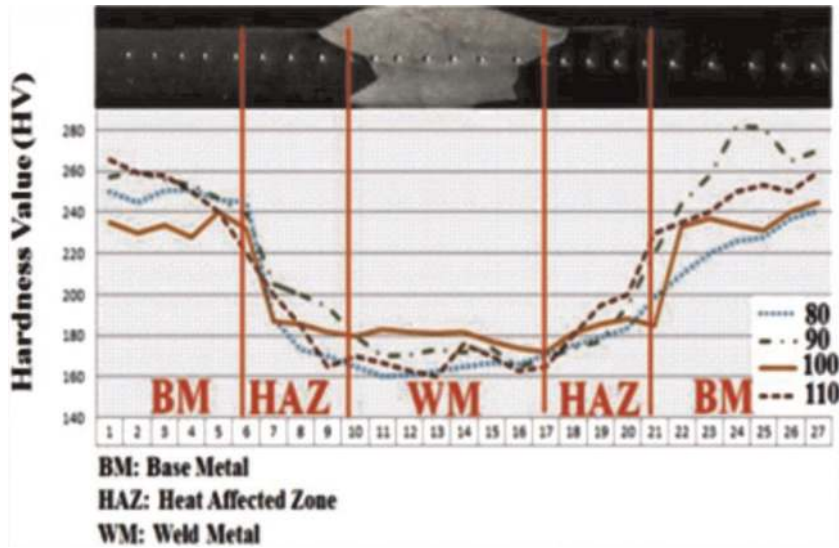


Figure 3. Comparison of number of points versus hardness (HV) of 316 stainless steel welded joint.

Ar + 3% N<sub>2</sub>, 94%Ar + 6%N<sub>2</sub>, and 91%Ar + 9% N<sub>2</sub> for welding 2205 DSS using TIG welding. The austenitic structure increased with increasing N<sub>2</sub> content in shielding gas (Figure 4). Increasing N<sub>2</sub> content in argon shielding gas led to improve grain size, UTS and HV of DSS welds (Figure 5).

Besides that, Mosa et al. [12] studied the effect of shielding gas and heat input on mechanical properties of ASS 304 L welded by TIG welding. Tensile strength and hardness values decrease with increasing heat input, but the ferrite number, impact toughness, penetration depth and weld bead width increase. Addition of N<sub>2</sub> in Ar increases UTS and HV but reduces FN and impact toughness (Figures 6–11).

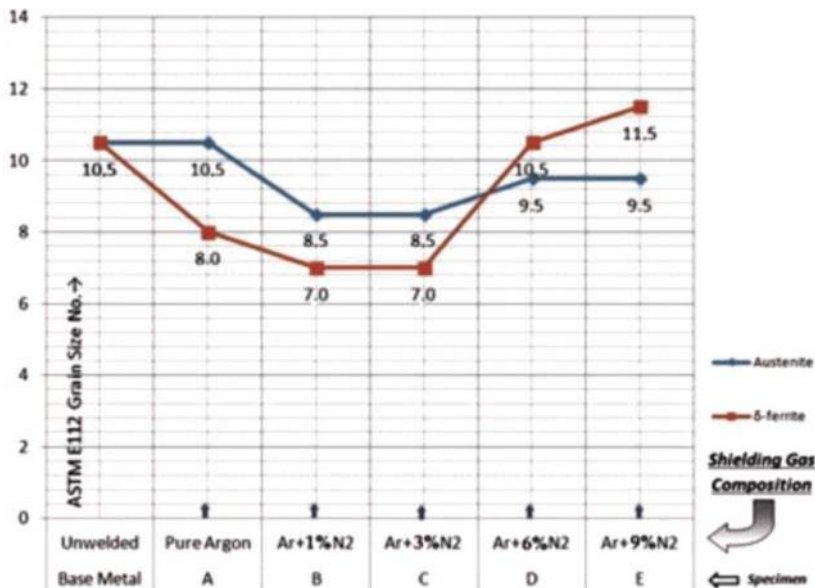


Figure 4. The effects shielding gas composition on phases grain size.

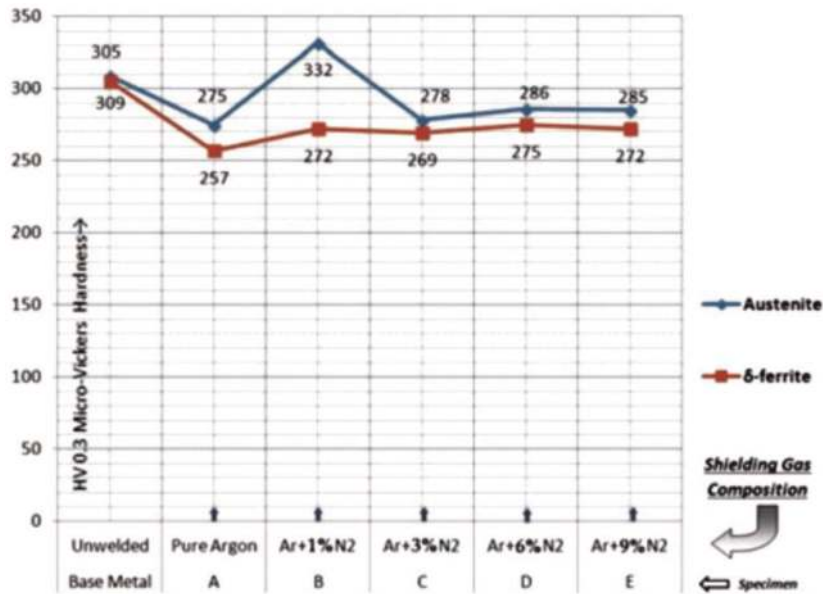


Figure 5. The effects of shielding gas composition on micro-hardness values of base metal and weldments.

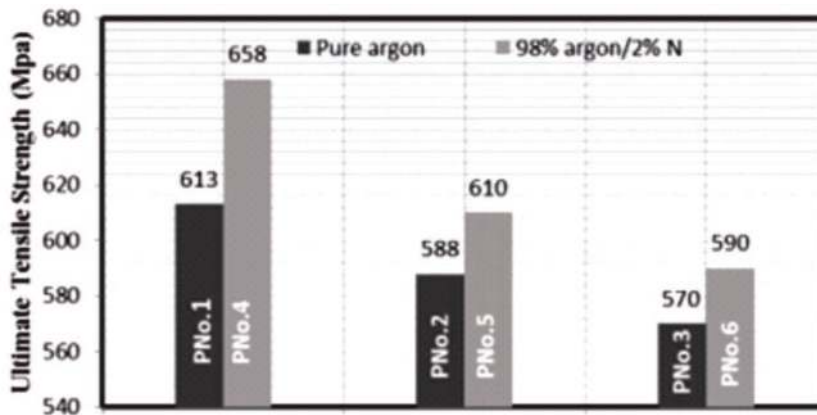


Figure 6. Comparison between ultimate tensile strength of welding procedures using shielding gas pure Ar and 2%N/98%Ar.

### 2.1.3 Welding speed

Welding speed is the linear speed at which the arc moves with respect to the plate, along with the weld joint. The heat input and cooling rate increase with decreasing welding speed. Welding speed is calculated by Eq. (2) [13]:

$$\text{Welding Speed (mm/min)} = \text{Electrode Travel/Arc Time} \quad (2)$$

Moreover, optimization of AISI 316 weld sample characteristics was studied [14] by Taguchi method (ANOVA). Besides, the effect of welding variables as welding speed and current, filler metal and root gap on UTS and bend strength was studied. Travel speed (46.51% contribution) has a greater influence on toughness (bend

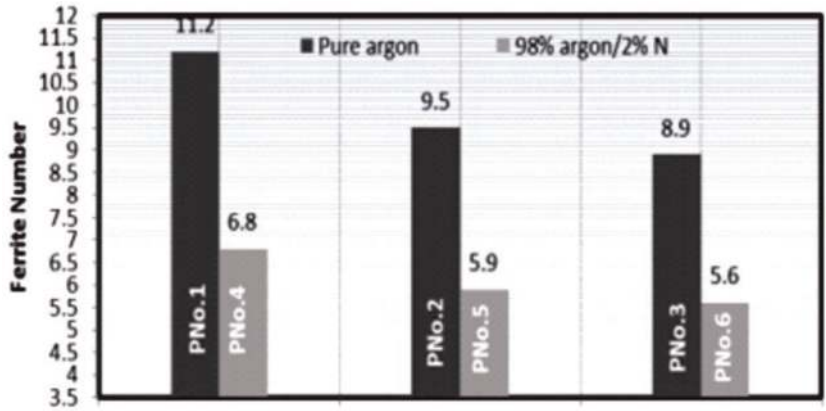


Figure 7. Comparison between FN of welding procedures using shielding gas pure and 2% N/98%Ar.

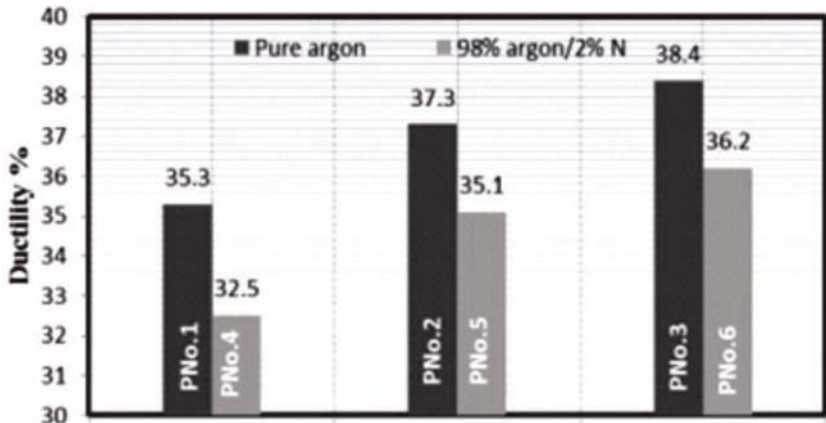


Figure 8. Comparison between ductility of welding procedures using shielding gas pure Ar and 2%N/98%Ar.

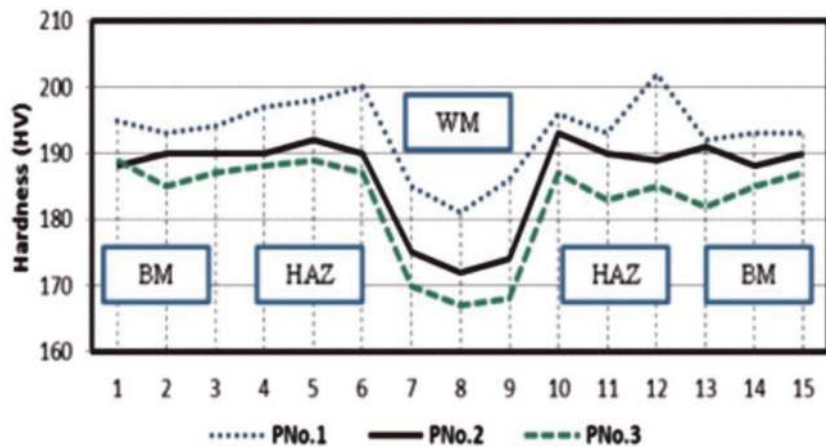
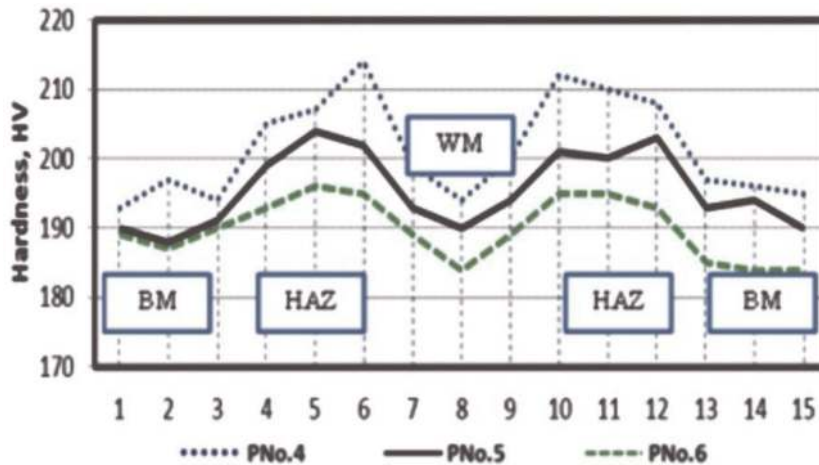
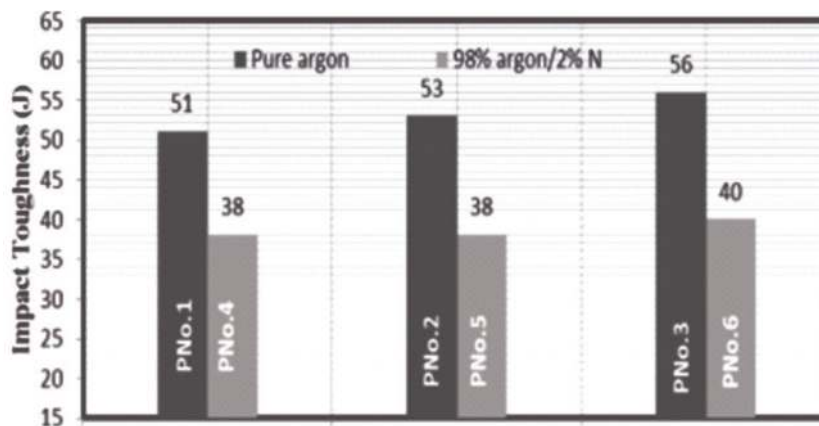


Figure 9. Hardness values for PNo.1 (0.395 Kj/mm), PNo.2 (0.79 Kj/mm) and PNo.3 (0.998 Kj/mm) all with using shielding gas of pure argon.



**Figure 10.** Hardness values for PNo.4 (0.411 KJ/mm), PNo.5 (0.822 KJ/mm) and PNo.6 (1.053 KJ/mm) all with using shielding gas of (2%N/98% Ar).



**Figure 11.** Comparison between impact toughness of PNo.3 versus PNo.4.

strength) and welding current (96.75%) has maximum influences on UTS. The root gap has some effect on both tensile and bend strengths.

#### 2.1.4 Effect of heat input

Heat input is a relative measure of the energy transferred per unit length of weld. It is an important characteristic because, like preheat and interpass temperature, it influences the cooling rate, which may affect the mechanical properties and metallurgical structure of weld region and HAZ [15]. It is calculated by Eq. (3).

$$HI \text{ (KJ/mm)} = \eta * (V * I * 60) / (S * 1000) \quad (3)$$

where HI is the heat input (in KJ/mm),  $\eta$  is welding efficiency ( $\eta_{TIG} = 70\%$ ), V is arc voltage (in volt), I is welding current (in Amp) and S is welding speed (in mm/min).

The effect of heat input on microstructure and mechanical properties have been extensively investigated. For example, Movahedi and Ozlati [16] studied the influence of heat input on mechanical properties of dissimilar welds AISI 410 MSS and 2209 DSS rods. The heat input, UTS and %EL increase with increasing welding current. Best results of UTS and %EL are obtained at a welding current of 3.5 kA. Whereas the lowest results of UTS and %EL are obtained at a welding current of 2 kA (Figure 12). Moreover, Sergei Yu et al. [17] analyzed the influence of  $H_{net}$  on residual strain and phase content in AISI 304 stainless steel welds using different heat input values. The ferrite content increased with increasing heat input from 0.225 to 0.247 kJ/mm, while the austenite content decreased.

Singh and Kumar [18] investigated the characteristics of 304 stainless steel joints using SMAW-GTAW hybrid welding and different filler metals. The joint with 90A

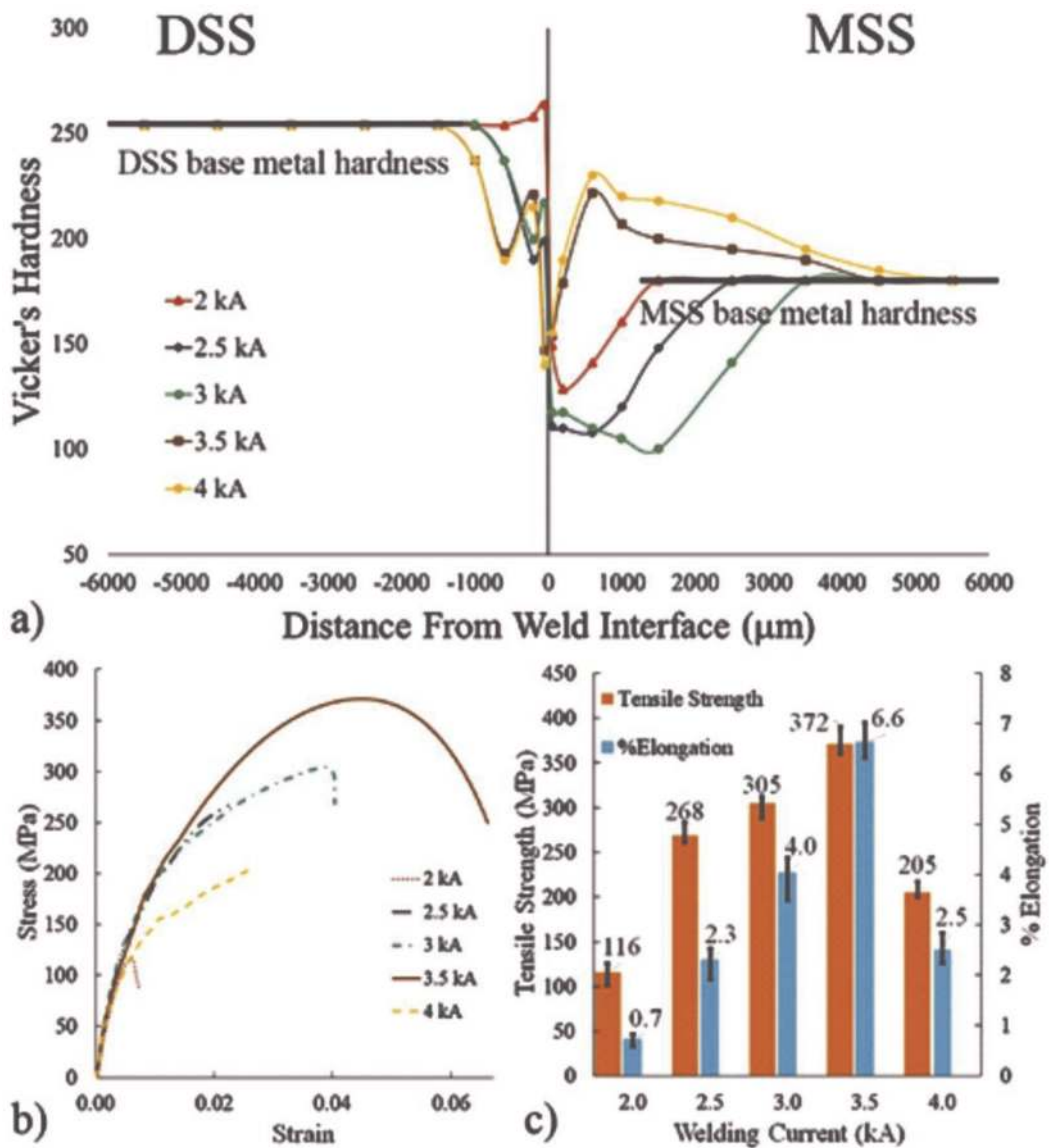


Figure 12. (a) Hardness profile across the weld interface. (b) Stress-strain curves and (c) values of tensile strength and elongation for all samples [16].



has the highest hardness value and lowest toughness value. The toughness value of weld metal and HAZ increases with increasing heat input. Welding width and depth (penetration) increase with increasing heat input. It can be seen that root reinforcement deposited at 0.93 kJ/mm is wider than that deposited at 0.68 kJ/mm. Whereas, D. Bahar [19] studied the effect of welding parameters as; welding current, gas flow rate and welding speed on bending strength and weld geometry of dissimilar welds of SS 304 and mild steel 1018. The welding width, depth of penetration and bending strength increased with increasing welding current, gas flow rate and welding speed. Additionally, Bodude and Momohjimoh [20] explained the influence of welding variables on mechanical properties of low carbon steel welded by SMAW. Highest ultimate tensile strength and hardness were realized for samples welded at low current. Moreover, best results of weld toughness were obtained at welding current of 150A. HV and UTS increased with decreasing heat input, while the impact toughness increased with increasing heat input. Gupta et al. [21] studied the influence of  $H_{net}$  on the mechanical behavior of FSS 409 plate using two different filler metals (ER304L and ER308 L). Best UTS result, yield strength, hardness value and grain size is obtained using medium heat input '4 kJ/mm', irrespective of the used filler metal. The mechanical behavior is also influenced by grain size of weld metal and heat input. Generally, the joints welded using 304 filler metal showed better results than using 308 filler wire. Moreover, the effect of heat input on the mechanical properties and fatigue life of AA6061 alloy welded by MIG welding was reported [22]. The weld penetration increased linearly with increasing the weld current and arc voltage, but with decreasing the welding speed. On the other hand, the fatigue life decreased with increasing the welding current and arc voltage, whereas, the fatigue life increased with increasing the welding speed. The impact toughness increased slightly with increasing heat input (**Table 1**). Swami et al. [23] studied the influence of MIG welding current, gas flow rate and shielding gas on UTS of 12 mm thick mild steel plates. MIG welding process variables affect UTS value of the weld metal. Best UTS result was recorded at 190 A, 15 (L/min) and 50% CO<sub>2</sub>. Bansod et al. [24] investigated the change of mechanical properties of low-nickel ASS 304 welds using SMAW technique at various heat input values. Highest UTS and HV were obtained using low heat input values (**Table 2**). Hardness of the weld zone was lower than that of the heat affected zone and base metal (**Figures 13–15**). The ferrite number of weld region increased with decreasing the heat input (**Table 3**). Furthermore, Bansod et al. [25] studied the influence of heat input on physical metallurgy, mechanical behavior and corrosion rate of Cr-Mn ASS and low nickel ASS specimens. The width of HAZ increased with increasing heat input, while the FN and volume fraction of delta ferrite in weld region decreased. On the other hand, the hardness and tensile strength increased with decreasing heat input. Besides, the pitting resistance was improved with increasing delta ferrite. Ahmed et al. [26] studied the change of weld strength of ASS 316 welds using GTAW technique at various heat input values and filler metals. Using ERNiCrMo-3 as filler rod produced weldments with higher ultimate tensile strength and yield stress than using ER309L or ER316 L. The ultimate tensile strength, yield stress and elongation percent decrease with increasing heat input. Highest values are obtained using ERNiCrMo-3 filler rod at comparatively low welding current (80 A). The hardness is lower in weld zone than that of in heat affected zone and base metal. In general, it decreases with increasing heat input (welding current). Highest values are obtained using ERNiCrMo-3 filler with low heat input (80 A) (**Figures 16–18**).

Sample number	Heat Input (J/mm)	No. of cycles to failure	Impact energy (J)	Penetration (mm)
1	264	221	83.91	2.411
2	219.96	360	67.37	2.464
3	188.58	476	47.71	2.310
4	303.6	198	91.27	2.571
5	252.96	331	73.75	2.612
6	216.84	463	55	2.511
7	343.2	161	91.25	2.599
8	285.96	317	83.93	2.634
9	245.1	429	71.6	2.541
10	312	190	94.18	2.781
11	259.98	325	83.01	2.872
12	222.84	439	67.63	2.741
13	358.8	157	81.41	2.860
14	298.98	296	90.55	2.932
15	256.26	408	77.21	2.802
16	405.6	101	63.25	2.941
17	337.98	264	94.32	2.970
18	289.68	372	84.62	2.872
19	360	136	77.84	2.983
20	300	272	91.01	3.020
21	257.1	390	78.68	2.911
22	414	98	61.17	3.078
23	345	258	85.65	3.101
24	295.68	366	88.61	3.001
25	468	85	58.64	3.150
26	390	246	71.91	3.202
27	334.26	353	93.65	3.120

**Table 1.** Life, impact energy and penetration of weld with respect to the weld parameters [22].

### 2.1.5 Cooling rate and solidification time

Cooling rate ‘CR’ is the heat loss during welding per unit time. CR plays an important role in determining the final solidification microstructure and its properties. Merchant Samir [27] studied the influence of welding current, arc voltage and welding speed on cooling rate, solidification time and hardness value of mild steel welded by MMAW process. It was found that the cooling rate decreased with increasing the welding current, while the solidification time increased for samples welded using different current and voltage values. The cooling rate increased with increasing

	Base metals		Dissimilar joint welded by different fillers		
	Cr-Mn SS	304 SS	316 L	310	308 L
Yield strength (MPa)	222.6	335.2	336.7	330.4	333.3
Ultimate tensile strength (MPa)	808.7	670	667.50	660.0	667.9
% elongation	60.2	52.5	50.34	49.5	55.2
Fracture zone	—	—	304	304	304

**Table 2.**  
 Tensile test results [24].

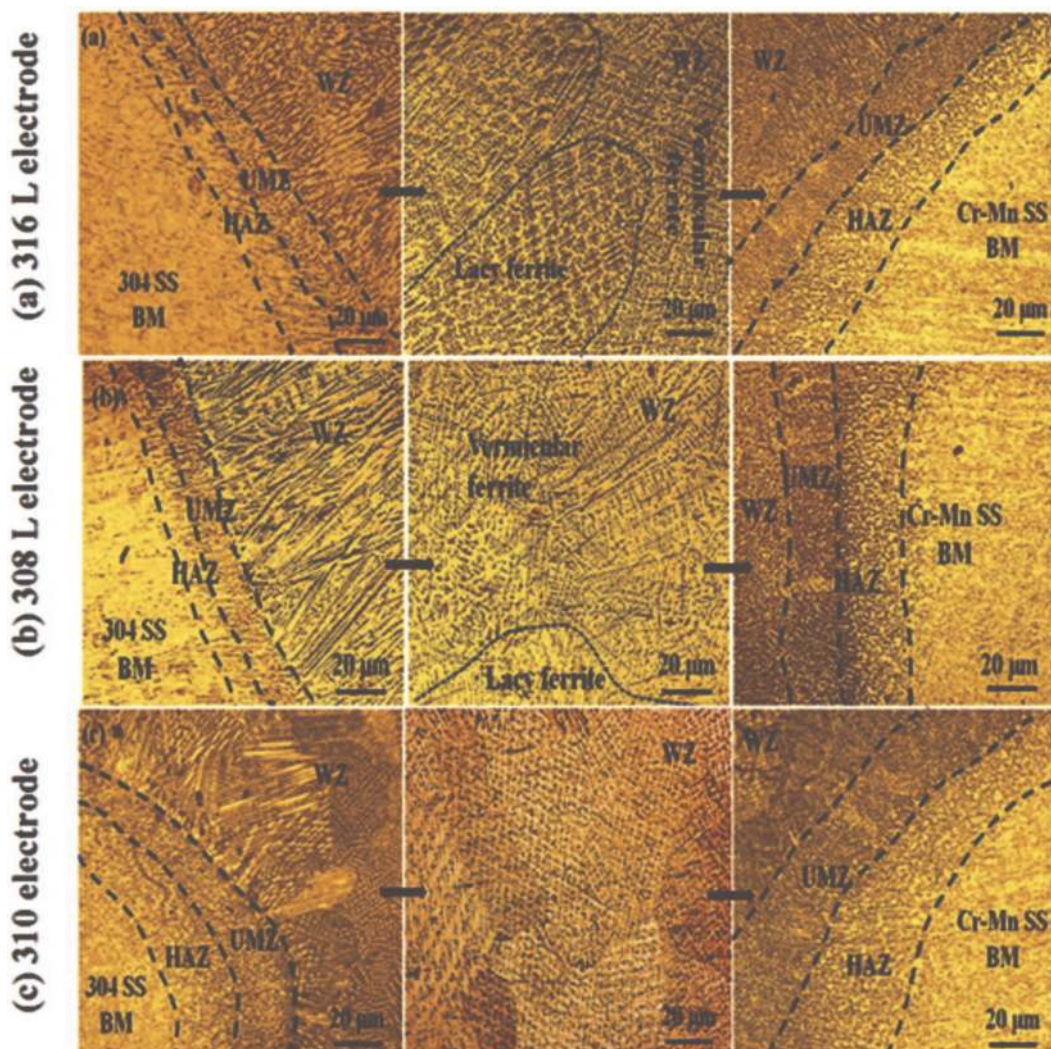


**Figure 13.**  
 Optical micrographs of weld samples (a) 316 L electrode, (b) 308 L electrode and (c) 310 electrode [24].

welding speed, while the solidification time decreased. The best result for *HRN* is obtained in HAZ of all samples. Besides, Rahul Kumar et al. [28] examined the effect of welding variables and cooling rate on the mechanical behavior of mild steel welded by SAW. They found that the cooling rate and hardness increased with reducing the

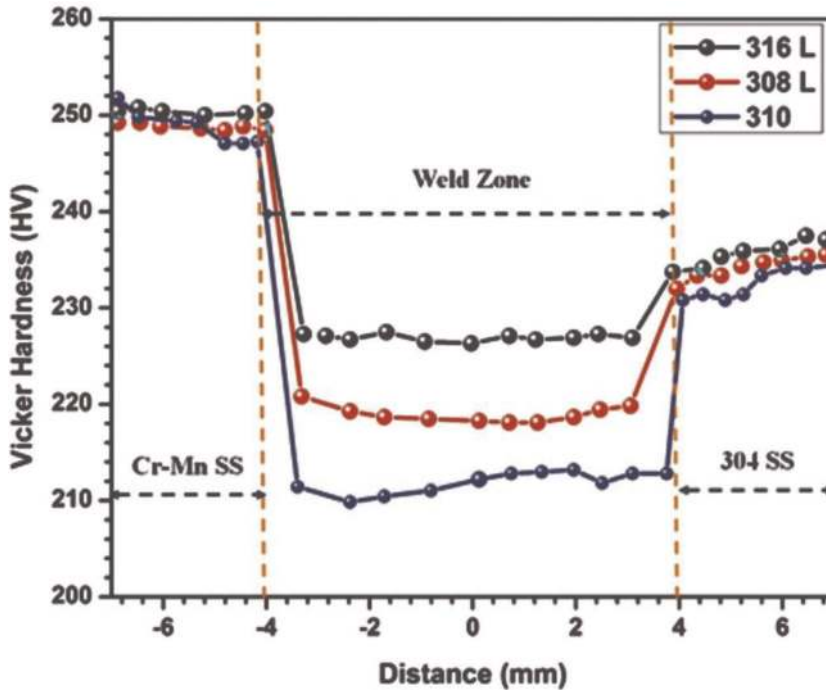


Figure 14. Microhardness profile across the weld specimens [24].

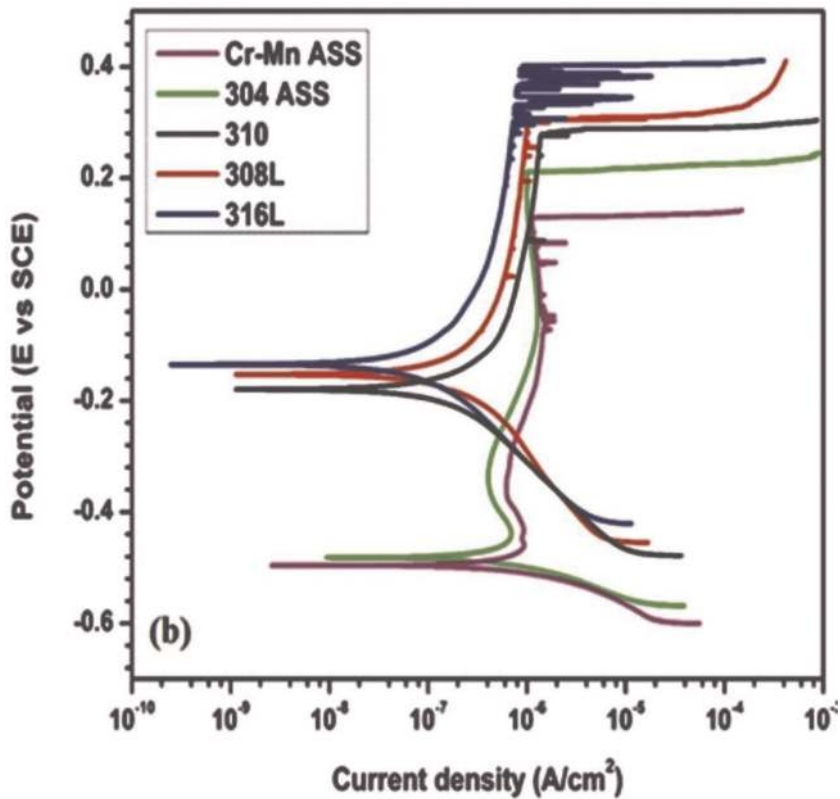
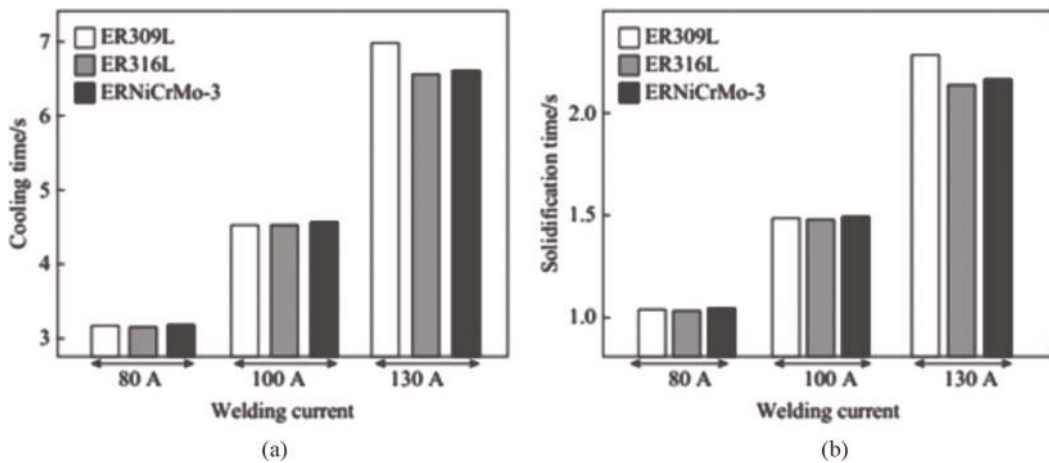


Figure 15. Potentiodynamic polarization plots of various sample [24].

Welding Electrodes	Unmixed zone length (μm) 304 SS	HAZ width (μm)	Unmixed zone length (μm) Cr-Mn SS	HAZ width (μm)	Average level of dilution (%)	δ-ferrite by Ferritoscope (FN)		
						Weld zone	Base metal (304 SS)	Base metal (Cr-Mn SS)
316 L SS	180	245	257	498	24 ± 3	6.0	0.15	0.16
308 L SS	181	240	250	452	25 ± 3	5.1	0.15	0.16
310 SS	185	256	255	468	24 ± 2	0.14	0.15	0.16

**Table 3.**  
 Microstructural details of welding [24].



**Figure 16.**  
 Effect of welding current on (a) cooling time (b) solidification time of 316SS welding [26].

heat input. Whereas a finer grain size was formed at higher cooling rate and lower heat input.

Effect of cooling rate on solidification and segregation characteristics of SASS was studied [9]. The grain size was refined more with increasing cooling rate. Dendrite arm spacing decreased at welding begin, then decreased slowly with increasing cooling rate. Transition cooling rate was 20°C/sec. Also, the effect of heat input on cooling rate and PREN in SDSS welds was studied [14]. Grain size and cooling rate increased with increasing heat input. Best results for PREN were obtained at an intermediate heat input value of 1.4 kJ/mm. Besides, Ahmed et al. [29] examined the effect of heat input and shielding gas on the Performance of 316SS welded by GTAW. They found that the heat input, cooling time, solidification time, grain size and nugget area increase with increasing the welding current. Besides, the cooling rate decreases with increasing the welding current. Whereas the UTS, YS and EL% decrease with increasing heat input, and the addition of 2% N<sub>2</sub> to Ar shielding gas increases the mechanical properties of 316 stainless steel weld joints. The best mechanical properties are obtained at welding current 80 amp with Ar-2%N<sub>2</sub>. The hardness is lower in the weld zone than in the heat affected zone and base metal, and the addition of 2% N<sub>2</sub> to shielding gas increases it. Moreover, the hardness decreases with increasing heat input (Figures 19–26).

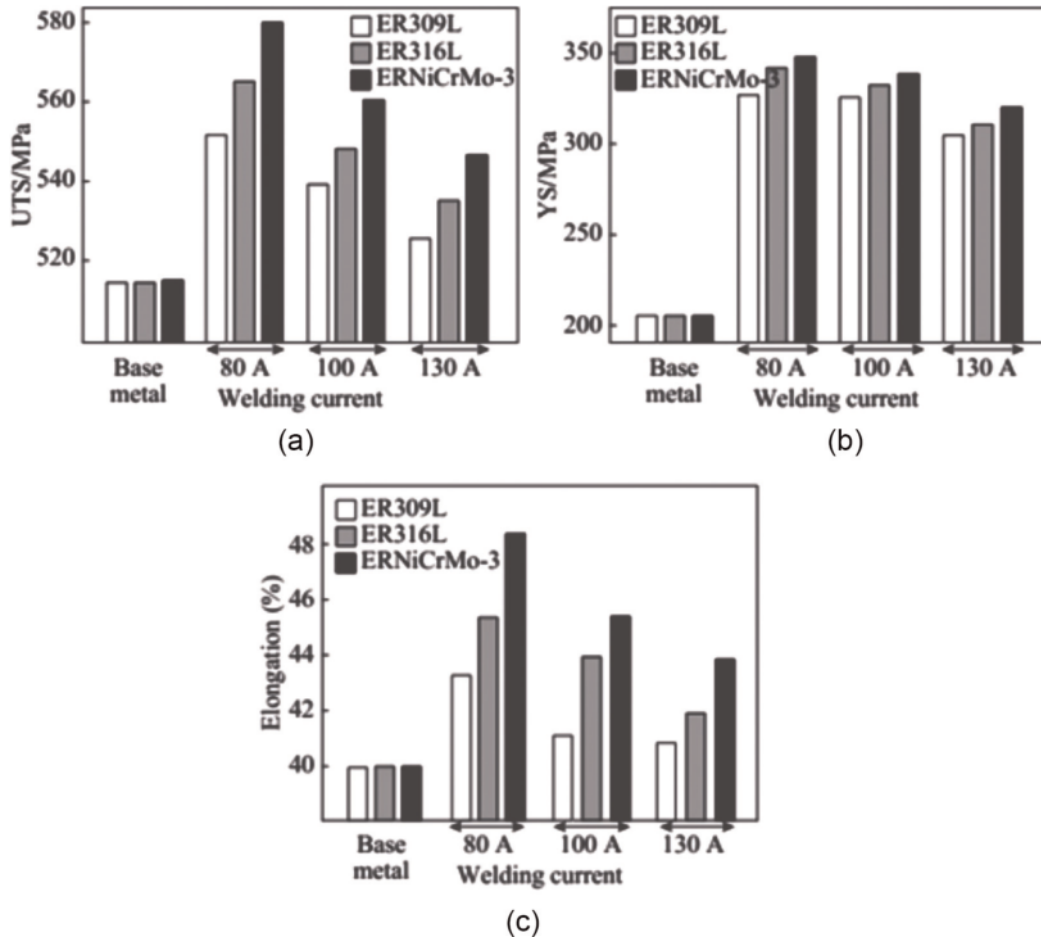


**Figure 17.** Mechanical test results of TIG welded joints (a) tensile strength, (b) yield strength, and (c) percentage elongation [26].

The cooling rate in the temperature range 800–500°C is important for phase transformation of stainless steel. It determines the final solidification mode or microstructure of the weld metal and its properties [30]. The cooling rate and cooling time [26, 31] can be calculated using Eq. (4) and Eq. (5), respectively.

$$\left(\frac{\partial T}{\partial t}\right)_x = \left(\frac{\partial T}{\partial x}\right)_t * \left(\frac{\partial x}{\partial t}\right)_{xT} = -2\pi K * \left(\frac{(T - T_o)^2}{H_{net}}\right) \quad (4)$$

$$t_{8_5} = \frac{HI}{2\pi\lambda} * \left(\frac{1}{500 - T_o} - \frac{1}{800 - T_o}\right) \quad (5)$$

where,  $(\partial T/\partial t)_x$  is the cooling rate ‘°C/sec’,  $K$  or  $\lambda$  is the thermal conductivity (W/mmK), and  $T$  is the temperature near the pearlite nose on TTT diagram ‘550°C’ and  $T_o$  is the initial temperature of the plate ‘20°C’.

The solidification time ‘ $S_t$ ’ of welding joint depends on the cooling rate and heat input. The  $S_t$  time is important as it affects the microstructure and properties, and can be calculated using Eq. (6) [26, 31]:

$$St \text{ (sec)} = L H_{net}/2\pi K\rho c (T_m - T_o)^2 \quad (6)$$

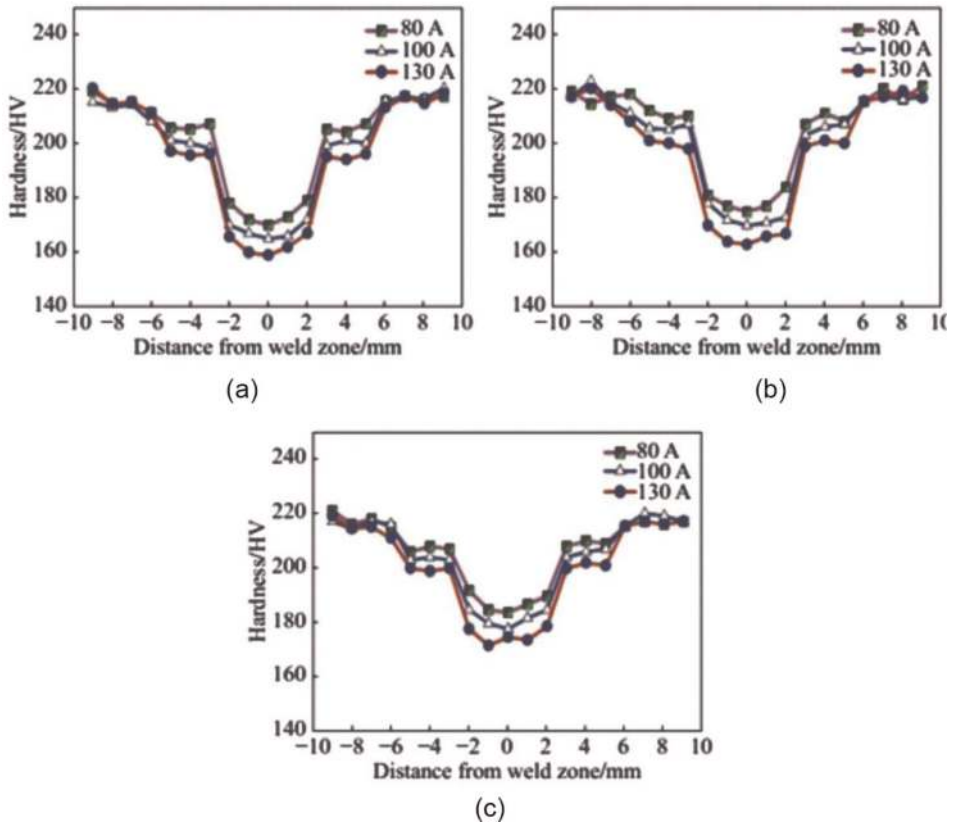


**Figure 18.** Vickers hardness profiles of 316SS TIG joint cross sections for different values of welding current using (a) ER309L, (b) ER316 L and (c) ERNiCrMo-3 as filler rods [26].

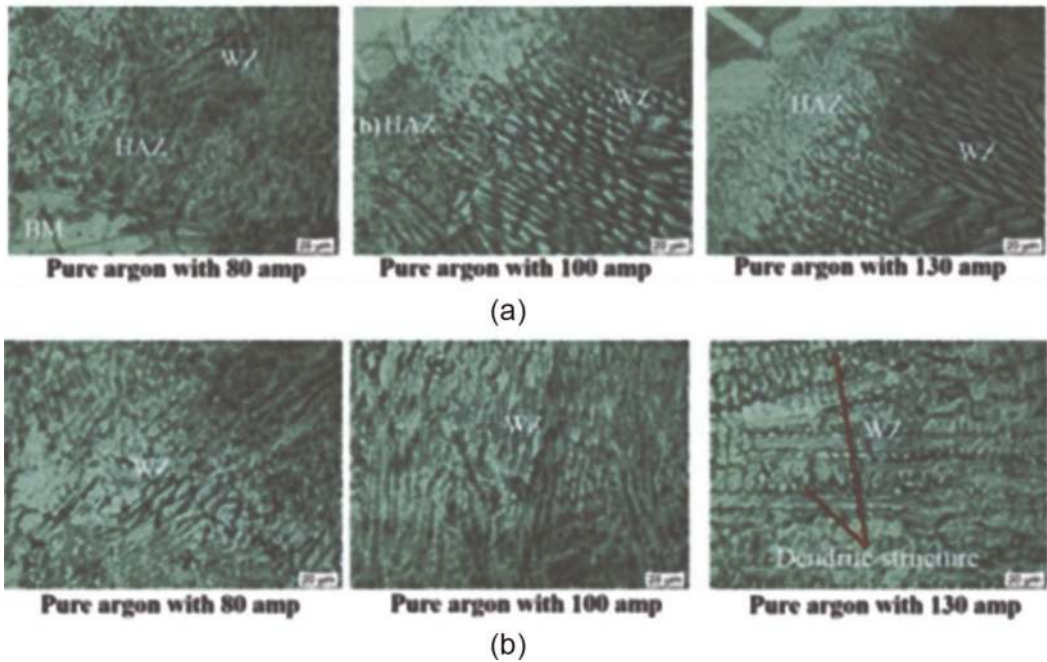


**Figure 19.** Microstructure of weldments using various welding currents 80, 100 and 130 amp and pure argon as shielding gas, at different locations (a) and (b) [31].

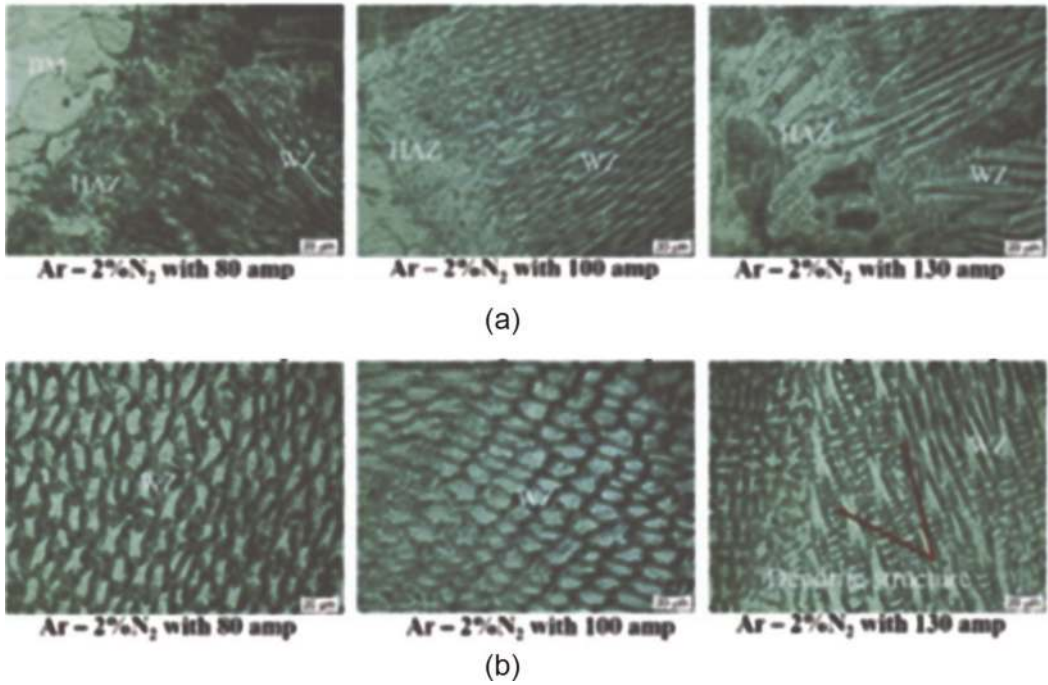


**Figure 20.** Microstructure of weldments using various welding currents 80, 100 and 130 Amp and Ar-2%N<sub>2</sub> as shielding gas, at different locations (a) and (b) [31].

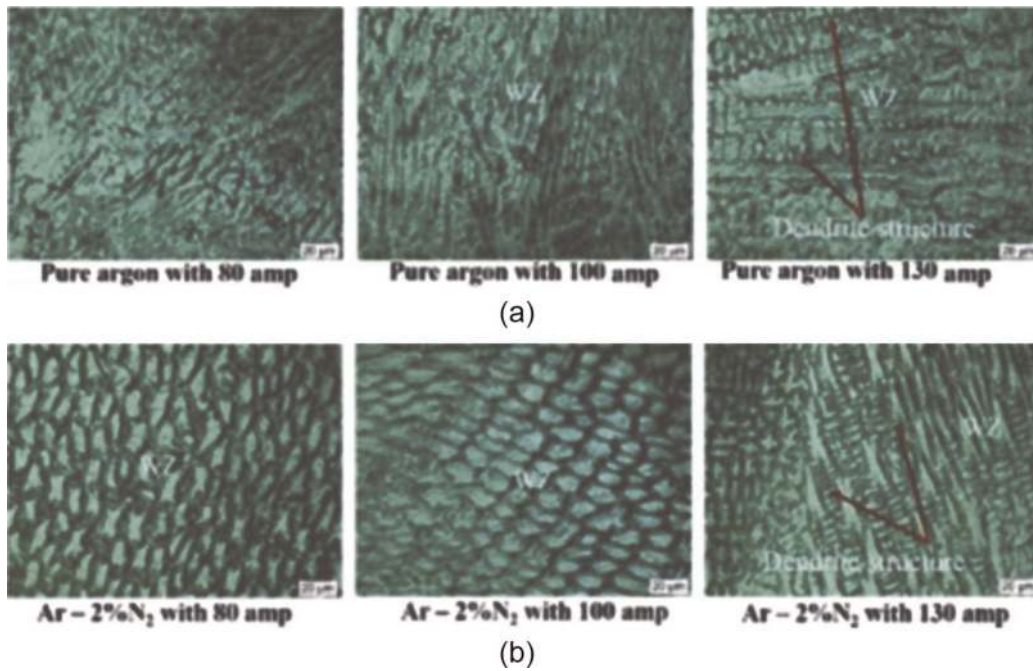


**Figure 21.** Microstructure of weldments using various welding currents 80, 100 and 130 amp with/without N<sub>2</sub> [31].

### 2.1.6 Weld bead geometry

The effect of weld bead area on mechanical properties was investigated [26, 31], and it was found that the nugget area 'Na' increases with increasing weld current and



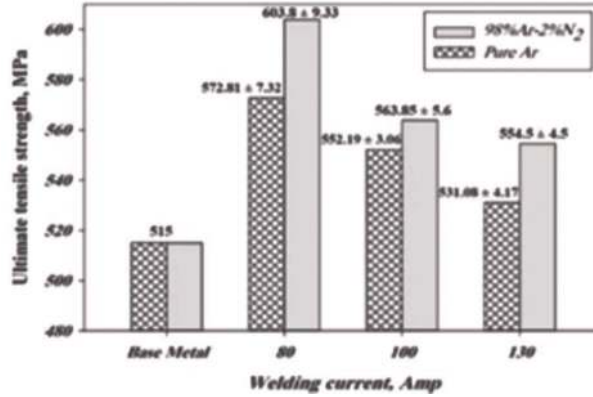


**Figure 22.** Ultimate tensile strength of GTAW welded AISI 316SS using various welding currents 80, 100 and 130 Amp and Ar-2%N<sub>2</sub> as shielding gas [31].

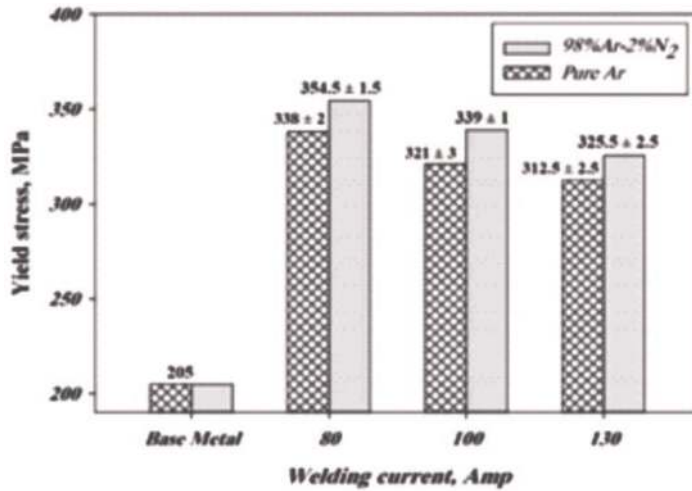


**Figure 23.** Yield stress of GTAW welded AISI 316SS using various welding currents 80, 100 and 130 Amp and Ar-2%N<sub>2</sub> as shielding gas [31].

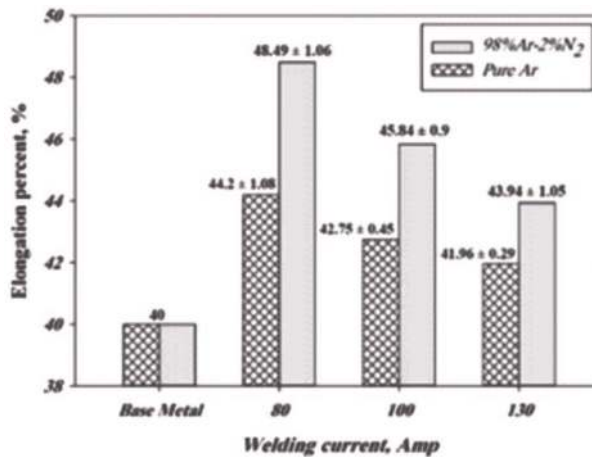


**Figure 24.** Percentage elongation of 316SS welding specimens [31].

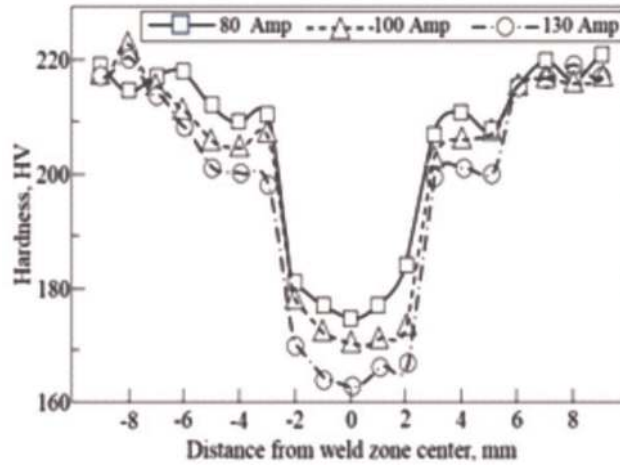


**Figure 25.**  
Hardness profiles of 316SS GTAW joint cross sections of weld joints using pure argon as shielding gas [31].

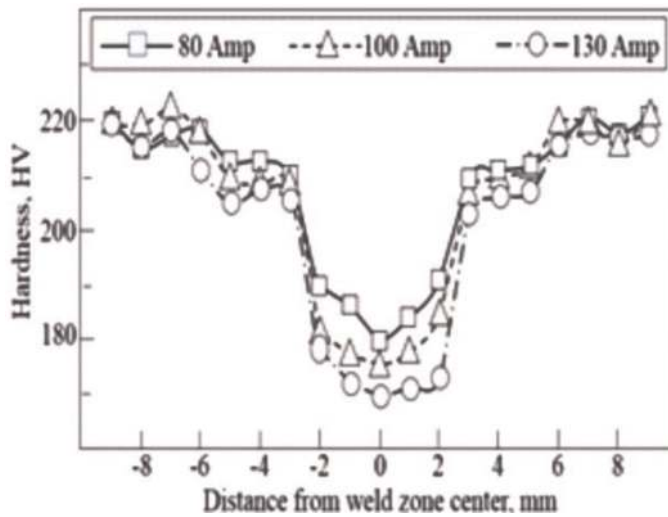


**Figure 26.**  
Hardness profiles of 316SS GTAW joint cross sections of weld joints using Ar-2% N<sub>2</sub> as shielding gas [31].

arc voltage, but decreases with increasing welding speed, and can be calculated with Eq. (7) (Table 4).

$$Na \text{ (mm}^2\text{)} = 33312 * 10^{-6} * [A1.55/S0.903] \quad (7)$$

where, Na is nugget area 'mm<sup>2</sup>', A is the welding current in 'amp', and S is the welding speed 'mm/sec'.

### 3. Conclusions

1. Increasing weld current, increases heat input, time of cooling and of solidification, metal deposition rate and nugget area, but decreases cooling rate.

Weld current	Electrodes	Nugget area
80 amp	ER309L	17.3
100 amp		26
130 amp		42.4
80 amp	ER316 L	17.2
100 amp		26
130 amp		40
80 amp	ERNiCrMo-3	17.4
100 amp		26.2
130 amp		40.3

**Table 4.** Nugget weld area of 316SS specimens welded using different welding current values and filler metals and pure Ar shielding gas [26].

2. Ultimate tensile strength, yield stress, elongation percent and fatigue life decrease with increasing weld current. Using ERNiCrMo-3 filler rod, 80amp weld current and 2%N<sub>2</sub> in shielding gas leads to highest mechanical properties.
3. The hardness is lower in weld zone than in heat affected zone and base metal. The addition of 2% N<sub>2</sub> to shielding gas increases it, but the increase of weld current decreases it. Using ERNiCrMo-3 filler rod, 80 amp weld current and 2% N<sub>2</sub> in shielding gas leads to highest hardness.
4. Weld metal grain size and crystallization temperatur increase with increasing heat input and N<sub>2</sub> content in the shielding gas. Adding 2% N<sub>2</sub> to Ar shielding gas leads to  $\alpha \rightarrow \gamma$  phase transformation.
5. Average size of secondary dendrite arm spacing and eutectic volume fraction increase with decreasing cooling rate. At lowest cooling rate “31.5°C/s” the volume fraction is ~1.96%.
6. Using ER309L filler rod leads to higher toughness, and adding 2%N<sub>2</sub> to Ar shielding gas leads to lower toughness, that increases with increasing weld current, and decreasing N<sub>2</sub> in shielding gas.
7. From the mathematical modeling, by adding 2%N<sub>2</sub> to shielding gas UTS, HV and spattering increase. While UTS, HV and spattering decrease with increasing the welding current.

## Acknowledgements

The success of this research has been achieved due to the invaluable contributions of various individuals. I would like to take this opportunity to acknowledge their efforts:

I would also like to express gratitude to the headmaster of Petrojet Company (Suez) for providing welding process and collaboration.

Furthermore, I want to thank all my friends who gave me a wonderful time to support me to finish this chapter, especially, Dr. Eng. Ahmed M. Fouad, Dr. Asmaa Fouad, Dr. Fadel Shaaban, Dr. Waheed S. A. Barakat and Dr. Mohamed I. Habba. I would like to wish them all good luck in their further carrier, and of course. I hope we remain friends.

## **Author details**

Ramy A. Fouad<sup>1\*</sup>, Essam Ahmed Ali<sup>2\*</sup>, Ahmed Ramadan Shaaban<sup>1\*</sup>  
and Ahmed E. El-Nikhaily<sup>3\*</sup>

1 Mechanical Department, Faculty of Technology and Education, Suez University, Egypt


2 Metallurgical and Materials Engineering, Faculty of Petroleum and Mining Engineering, Suez University, Egypt

3 Metal Forming Engineering, Faculty of Technology and Education, Suez University, Egypt

\*Address all correspondence to: ramy\_fouad12@suezuniv.edu.eg;  
essam.ahmed@suezuni.edu.eg; ahmed.essa@suezuni.edu.eg;  
ahmed.eassa@ind.suezuni.edu.eg

## **IntechOpen**

---

© 2022 The Author(s). Licensee IntechOpen. This chapter is distributed under the terms of the Creative Commons Attribution License (<http://creativecommons.org/licenses/by/3.0>), which permits unrestricted use, distribution, and reproduction in any medium, provided the original work is properly cited. 

## References

- [1] Nabavi B, Goodarzi M, Amani V. Nitrogen effect on the microstructure and mechanical properties of nickel alloys. *Welding Journal*. 2015;**94**:53-60
- [2] Lin YC, Chen PY. Effect of nitrogen content and retained ferrite on the residual stress in austenitic stainless steel weldments. *Materials Science and Engineering*. 2001;**A307**(307):165-171. DOI: 10.1016/s0921-5093(00)01821-9
- [3] Yelamasetti B, Kumar S, Sridhar Babu B, Vishu Vardhan T, Gunda VR. Effect of filler wires on weld strength of dissimilar pulse GTA Monel 400 and AISI 304 weldments. *Materials Today: Proceedings*. 2019;**19**:1-5. DOI: 10.1016/j.matpr.2019.06.759
- [4] Bahador A, Hamzah E, Mamat MF. Effect of filler metals on the mechanical properties of dissimilar welding of stainless steel 316l and carbon steel A516 GR70. *Journal Teknologi (Sciences & Engineering)*. 2015:61-65. DOI: 10.11113/jt.v75.5174
- [5] Moslemi N, Redzuan N, Ahmad N, Hor TN. Effect of current on characteristic for 316 stainless steel welded joint including microstructure and mechanical properties. *12th Global Conference on Sustainable Manufacturing*. 2015;**26**:560-564. DOI: 10.1016/j.procir.2015.01.010
- [6] Bharatha P, Sridharb VG, Senthil Kumar BM. Optimization of 316 stainless steel weld joint characteristics using taguchi technique. *Procedia Engineering*. 2014;**97**:881-891. DOI: 10.1016/j.proeng.2014.12.363
- [7] Basyigit AB, Murat MG. The effects of TIG welding rod compositions on microstructural and mechanical properties of dissimilar AISI 304L and 420 stainless steel welds. *Metals*. 2018;**8**: 1-14. DOI: 10.3390/met8110972
- [8] Dhobale AL, Mishra HK. Review on effect of heat input on tensile strength of butt weld joint using MIG welding. *International Journal of Innovations in Engineering Research and Technology [IJIERT]*. 2015;**2**:1-13
- [9] Hao Y, Li J, Li X, Liu W, Cao G, Li C, et al. Influences of cooling rates on solidification and segregation characteristics of Fe-Cr-Ni-Mo-N super austenitic stainless steel. *Journal of Materials Processing Tech*. 2020;**275**:1-9. DOI: 10.1016/j.jmatprotec.2019.116326
- [10] Sameer SK. Study of influence of welding parameters on mild steel. *International Advanced Research Journal in Science, Engineering and Technology*. 2015;**2**:49-50. DOI: 10.17148/IARJSET.2015.2509
- [11] Basyigit AB, Kurt A. The effects of nitrogen gas on microstructural and mechanical properties of TIG welded S32205 duplex stainless steel. *Metals*. 2018;**8**:1-13. DOI: 10.3390/met8040226
- [12] Mosa ES, Morsy MA, Atlam A. Effect of heat input and shielding gas on microstructure and mechanical properties of austenitic stainless steel 304L. *International Research Journal of Engineering and Technology (IRJET)*. 2017;**4**:370-377
- [13] Suhail M, Hasan MF, Bharti PK. Effect of welding speed, current and voltage on mechanical properties of underwater welded mild steel specimen (C, Mn, Si) with insulated electrode E6013. *International Journal of Mechanical Engineering*. 2014;**4**: 120-124

- [14] Wang H-S. Effect of welding variables on cooling rate and pitting corrosion resistance in super duplex stainless weldments. *Materials Transactions, The Japan Institute of Metals*. 2005;**46**:593-601
- [15] Singh DK, Sahoo G, Basu R, Sharma V, Mohtadi-Bonab MA. Investigation on the microstructure-mechanical property correlation in dissimilar steel welds of stainless steel SS 304 and medium carbon steel EN 8. *Journal of Manufacturing Processes*. 2018;**36**:281-292. DOI: 10.1016/j.jmapro.2018.10.018
- [16] Movahedi M, Ozlati A. Effect of welding heat-input on tensile strength and fracture location in upset resistance weld of martensitic stainless steel to duplex stainless steel rods. *Journal of Manufacturing Processes*. 2018;**35**: 517-525. DOI: 10.1016/j.jmapro.2018.08.039
- [17] Sergei YT, Filippov AV, Savchenko NL, Fortuna SV, Rubtsov VE, Kolubaev EA, et al. Effect of heat input on phase content, crystalline lattice parameter, and residual strain in wire-feed electron beam additive manufactured 304 stainless steel. *The International Journal of Advanced Manufacturing Technology*. 2018;**99**: 2353–2363. DOI: 10.1007/s00170-018-2643-0
- [18] Randhawa HS, Kumar S. Effect of heat input on the characteristics of 304 austenitic stainless steel weld deposited by GTAW for root pass and SMAW for filler passes. *International Journal of Research in Advent Technology*. 2018;**6**: 1616-1621
- [19] Bahar D. Optimization of process parameters for tungsten inert gas (Tig) welding to join a butt weld between stainless steel (SS304) and mild steel (MS1018). *International Journal of Engineering Sciences & Emerging Technologies*. 2017;**10**:1-8
- [20] Bodude MA, Momohjimoh I. Studies on effects of welding parameters on the mechanical properties of welded low-carbon steel. *Journal of Minerals and Materials Characterization and Engineering*. 2015;**3**:142-153. DOI: 10.4236/jmmce.2015.33017
- [21] Gupta SK, Raja AR, Vashista M, Khan MZ, Yusufzai MZK. Effect of heat input on microstructure and mechanical properties in gas metal arc welding of ferritic stainless steel. *Materials Research Express*. 2018;**6**:1-17. DOI: 10.1088/2053-1591/aaf492
- [22] Ghazvinloo HR, Honarbakhsh-Raouf A, Shadfar N. Effect of arc voltage, welding current and welding speed on fatigue life, impact energy and bead penetration of AA6061 joints produced by robotic MIG welding. *Indian Journal of Science and Technology*. 2010;**3**:1-7
- [23] Swami SA, Jadhav SM, Deshpande A. Influence of Mig welding process parameters on tensile properties of mild steel. *European Journal of Engineering Research and Science*. 2016;**1**:1-5
- [24] Bansod AV, Patil AP, Moon AP, Shukla S. Microstructural and electrochemical evaluation of fusion welded low nickel and 304 ASS at different heat input. *Journal of Materials Engineering and Performance*. 2017;**26**:5847–5863. DOI: 10.1007/s11665-017-3054-3
- [25] Bansod AV, Patil AP, Shukla S. Effect of heat on microstructural, mechanical and electrochemical evaluation of tungsten inert gas welding of low-nickel ASS. *Anti-Corrosion Methods and Materials*. 2018;**65**:605–615. DOI: 10.1108/ACMM-05-2018-1941

[26] Ahmed E, Ahmed R, EL-Nikhaily A, Essa ARS. Effect of heat input and filler metals on weld strength of gas tungsten arc welding of AISI 316 weldments. *China Welding*. 2020;29:8-16. DOI: 10.12073/j.cw.20200107001

[27] Merchant Samir Y. Investigation on effect of heat input on cooling rate and mechanical property (hardness) of mild steel weld joint by MMAW process. *International Journal of Modern Engineering Research (IJMER)*. 2015;5: 34-41

[28] Kumar R, Arya HK, Saxena RK. Experimental determination of cooling rate and its effect on microhardness in submerged arc welding of mild steel plate (Grade c-25 as per IS 1570). *Journal of Material Sciences & Engineering*. 2014;3:1-4. DOI: 10.4172/2169-0022.1000138

[29] Ahmed R, Essa ARS, EL-Nikhaily A, Ahmed E. Effect of heat input and shielding gas on the performance of 316 stainless steel gas tungsten arc welding. *Journal of Petroleum and Mining Engineering*. 2020;22:9-15. DOI: 10.21608/jpme.2020.23038.1024

[30] Das D, Pratihar DK, Roy GG. Cooling rate predictions and its correlation with grain characteristics during electron beam welding of stainless steel. *The International Journal of Advanced Manufacturing Technology*. 2018;97:2241-2254. DOI: 10.1007/s00170-018-2095-6

[31] Ahmed R, Essa ARS, EL-Nikhaily A, Ahmed E. Effect of heat input and shielding gas on the performance of 316 stainless steel gas tungsten arc welding. *Journal of Petroleum and Mining Engineering*. 2020;22:9-15. DOI: 10.21608/jpme.2020.23038.1024